

Design description of silicon micro-machined cavity coupled far-infrared bolometer array

Gert de Lange, Michael D. Audley, Geert Keizer, Stephen Doherty and Colm Bracken.

Abstract—We give a design description of a novel way to construct bolometer arrays out of pixels that consist of thermally isolated Silicon Nitride islands that are suspended with long and narrow SiN legs on a Si wafer. We use a multi-wafer approach that facilitates the use of extra pixels on underlying wafers that fill the "empty" spaces between adjacent pixels in a top wafer. In this way we can achieve both a low thermal conductivity and a high pixel packing density. The design is especially of interest for far-infrared bolometer arrays for space based astronomy applications that need extremely low thermal conductance, where pixel size easily can be as large as a few millimeters.

Index Terms— Antenna arrays, Bolometers, Infrared detectors, Micromachining.

I. INTRODUCTION

BOLOMETER arrays with a radiation absorber on a thermally isolated Silicon Nitride (SiN) island are widely used as detectors in astronomical observatories, with applications ranging from microwave to x-ray frequencies [1]. A key aspect in this is that a SiN membrane suspended on a Si wafer is very robust, even with the very thin (sub-) micron dimensions of the SiN legs that are used to create the thermal isolation of the island. Clean room processing allows for either wet (with KOH) or dry (Deep Reactive Ion Etching) etching to remove the Si carrier wafer at the position of the island. The responsivity of a bolometer scales as G^{-1} whereas the ultimate Noise Equivalent Power (NEP), determined by thermal fluctuation noise, is proportional to \sqrt{G} , where G is the thermal conductance of the SiN legs. For applications in background limited far-infrared space-based astronomy (like the SPICA SAFARI instrument) a detector NEP of order $10^{-19} \text{ W}/\sqrt{\text{Hz}}$ is required. Translating this into the required dimensions for the SiN legs results in a typical length of the legs of order 500-1000 μm [2], [3]. An example of a single pixel far infrared bolometer is shown in Figure 1 and an example of an array of bolometers is shown in Figure 2. It can be seen in Figure 2 that the absorbing area of the bolometers takes up only a small amount of the footprint of the array. Low NEP bolometer arrays like this have a very low filling factor in the focal plane, contrary to arrays (e.g. in the SCUBA-2 instrument [4]) that act more as a CCD type of filled array.

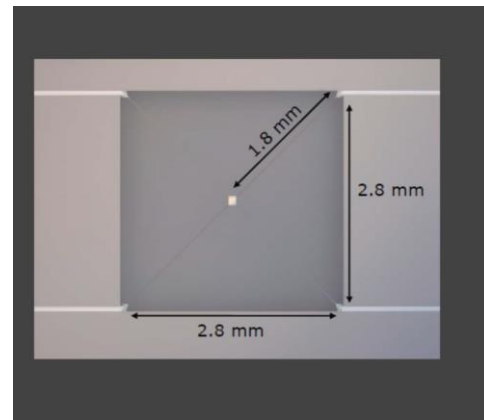


Figure 1 Example of typical low NEP $10^{-19} \text{ W}/\sqrt{\text{Hz}}$ bolometer design. The pixel to pixel spacing in this case would be at least 2.8 mm. The 1.8 mm arrow indicates the length of the SiN legs.

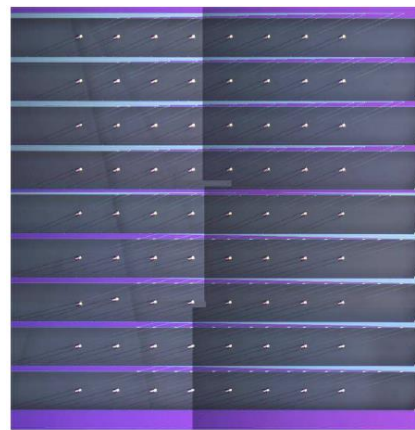


Figure 2 Example of a (wet etched) low NEP far-infrared bolometer imaging array. The light/dark color difference on the left and right side of this picture are due to photographic exposure. The array of light spots are the actual bolometers. As one can see only a small fraction of the area is actually covered by the active bolometers.

To improve the collecting area of the bolometers one typically places a light collecting horn in front of the bolometer array. This horn concentrates the light impinging on the front surface of the horn onto the much smaller bolometer area. With an array of light collecting horns and bolometers with long thin SiN legs, one can therefore build bolometer arrays with very low NEP values. However, the practical limitations to this are the dimensions of the resulting horn and bolometer array. With a typical pixel spacing of 1 to 2 mm (dictated by the required leg length) an array of 100x100 pixels would end up with an array size of say 15-25 cm. This can be prohibitively

large for single wafer processing and the design of cryogenic focal planes. To make better use of the available space in the focal plane we therefore propose to use a stack of bolometer wafers, where each wafer fills part of the empty space that is created by the long SiN legs of an overlying bolometer wafer. In order to optimize the radiation coupling to the individual bolometers, we propose to combine the bolometer wafers with a stack of micro-machined Si wafers that form a non-resonant cavity enclosing the bolometer. In this paper we show some initial design sketches of possible configurations of such an array, together with some initial results on simulations of the radiation coupling to the cavity enclosed bolometer arrays.

II. DESIGN DESCRIPTION OF A SINGLE LAYER CAVITY COUPLED BOLOMETER ARRAY.

Key to the designs described here is the use of Si DRIE etching of the bolometer and cavity wafers. Wet etching restricts the possible configuration of the design to the crystal planes within the wafer, but DRIE etching gives the possibility to etch any desired (vertical) shape within the wafer (see [5] for an application of Si micromachining to fabricate millimeter wave arrays). To illustrate the basic design of the proposed structure we first describe the design of a cavity enclosed single wafer bolometer. As a first step to reduce the pixel spacing we propose to make use of a triangular three leg suspension in a hexagonal packing, instead of a square four leg suspension. The reduction from four to three legs already reduces the thermal conductance and the hexagonal packing and DRIE etching gives the opportunity to have thermally overlapping pixels where a SiN leg of one pixel is placed into the footprint of an adjacent pixel. This is sketched in Figure 3 and Figure 4. For efficient coupling of far infrared radiation to the bolometer it is common to use a reflecting backshort at a distance of $\lambda/4$ behind the bolometer [4]. We propose to use an integrating cavity similar to bolometer designs described in [6] and [7]. A novel approach in this design is to build this cavity by mounting the bolometer wafer on a backing wafer that is etched such that part of the wafer close to the bolometer area is sticking through the bolometer wafer (where slits are etched at the position of the SiN legs). Another wafer with cavity sections and optical feed-throughs to the top surface of this wafer is placed on top to the bolometer and backing wafer. We then have an array of cavity coupled bolometers with optical access via a short section of waveguide or light-pipe. For radiation coupling to the waveguide one can use either a horn array or a Si micro-machined lens array placed in front of the wafer stack.

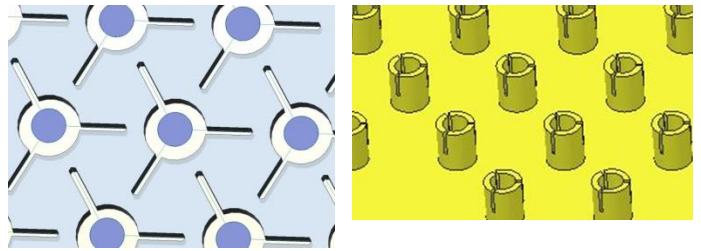


Figure 3 Left: Sketch of a hexagonally packed bolometer array fabricated with DRIE. The blue circles represent the thermally isolated islands that hold the absorber and the temperature sensor. The light blue area is the Si wafer. Electrical wiring to the devices is not shown. Right: The backing wafer where we have extruded the structure vertically in an exaggerated way to show the principle of operation. This backing wafer is made of Si that is fully gold plated

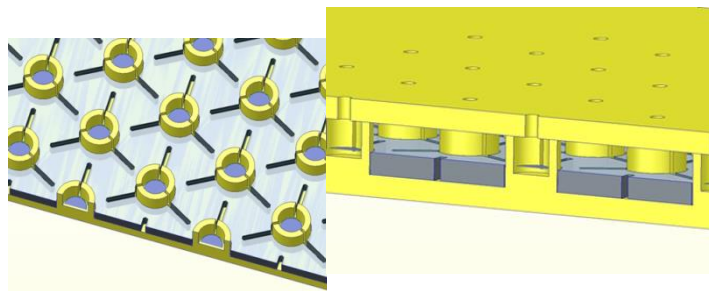


Figure 4 Sketch of a cavity enclosed bolometer array. The left figure shows how the bolometer wafer is placed on the backing wafer, where the lower wafer sticks through the bolometer wafer. Right: the sandwich of wafers including the top wafer (gold plated Si) that closes the cavity, but has an optical feedthrough to couple radiation into the cavity. Since the top wafer is not touching the surface of the bolometer wafer, the gold plated wafer will not short the bias lines of the bolometer wafer. A horn or lens array that is needed to focus the light into the light pipe is not shown.

III. DESIGN DESCRIPTION OF A MULTI-LAYER CAVITY COUPLED BOLOMETER ARRAY

To further enhance the packing density of the bolometers we propose to use the empty space in between the SiN legs. A sketch of this is shown in Figure 5 where the bolometer wafer and a backing wafer are shown.

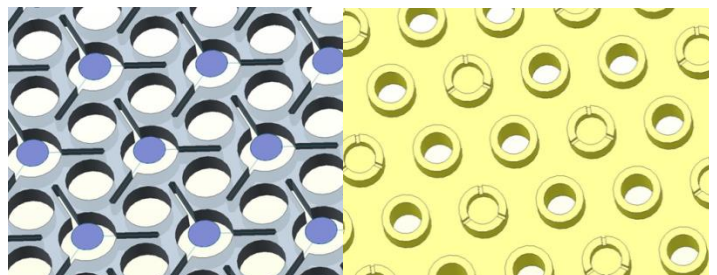


Figure 5 Left: Bolometer array with extra etched feedthroughs in between the SiN legs. Right: Backing wafer that contains cavities and feedthroughs.

With a stack of multiple wafers we can create a structure as shown in Figure 6 and Figure 7.

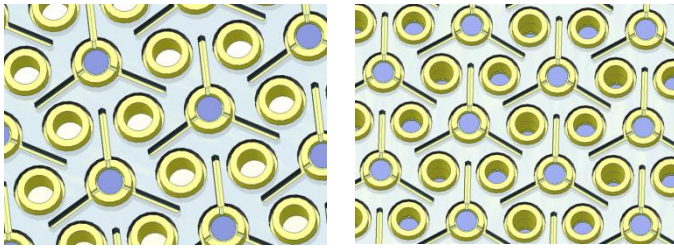


Figure 6 Left: first stage of assembly of a multi-wafer bolometer array. Right: final assembly of the hexagonally packed array. Note that the bolometers are at different depths within the cavity. The top wafer that closes the cavities is not shown.

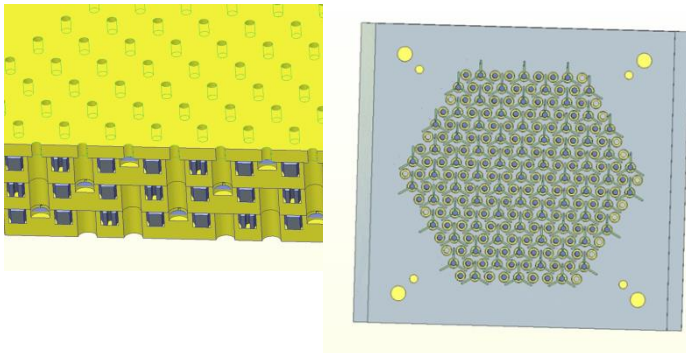


Figure 7 Left: side view of the multi-wafer bolometer design. The yellow wafers are gold plated Si wafers, the grey wafers are the Si wafers that hold the bolometers. Right: final assembly of the hexagonally packed array. The top wafer that closes the cavities is not shown. Details of the bias line connections at the side of the wafers are not shown in this sketch.

The bolometer array now consists of three layers of bolometers and 4 additional backing/topping wafers. If we take a fixed pixel-to-pixel spacing L_{pix} it can be shown that with this identical pixel spacing in a square array and an array as shown in Figure 7, the thermal conductance in the hexagonal array can be about a factor of three lower. For an array of Transition Edge Sensors therefore the phonon noise limited NEP can be reduced by a factor of $\sqrt{0.3}$, for an array that has the same physical dimensions as a square pixel design. If the array size is a design driver the hexagonal design can pack about a factor of 9 more pixels in the same area. This can be of great benefit in reducing the size of large number TES arrays.

IV. SIMULATED DEVICE RESPONSE

In the previous section we have sketched a possible configuration of a cavity enclosed bolometer, without detailing the actual design of the cavity. The absorbing material for far-infrared bolometers with $\lambda/4$ back-shorts generally consists of a thin semi-transparent metal film or mesh with a surface impedance close to 377 ohm (matching the free space impedance). This allows for a 100% coupling efficiency of incoming radiation to the absorber at the resonant wavelength. The general approach for the enclosed bolometers described here is that the cavity is over-moded for the wavelength of interest and is non-resonant, and therefore broadband. We basically propose to build a black-body type cavity with reflecting walls and an absorbing film as discussed by Richards and Winston [6],[7]. The exact position of the film within the cavity is not very critical, which is an

advantage over $\lambda/4$ back-shorts that have to be fabricated with μm accuracy at FIR wavelengths. At very short wavelengths (in a ray-tracing approach) such a cavity can be considered as a highly reflecting cavity with a free standing metal film, where light bounces from surface to surface and loses part of its energy at every pass through the absorbing film. So the radiation in the cavity is either absorbed by the film, or reflected out of the cavity via the entrance aperture. A cylindrical cavity as sketched previously would be possible, but we have simulated the response of square cavities that are terminated by a pyramid. The reason for this is that pyramidal cavities can be etched with an anisotropic KOH etch of Si $\langle 100 \rangle$ wafers [8] resulting in reflecting surfaces with extremely low surface roughness. A sketch of an array with pyramidal shaped cavities is shown in Figure 8. In a ray tracing approach the 70.6 degree angle of the etched pyramidal shape causes many reflections within the cavity, contrary to a flat surface or a 90 degree corner cube like reflector.

We have analyzed the pyramidal shaped cavity first with ZEMAX in a ray tracing method, which corresponds to a situation where the incoming light has a much smaller wavelength than the dimensions of the cavity structure. This is the extreme case of a multi-mode approach where a high number of electromagnetic modes is present [9]. As another extreme we have analyzed the structure with the COMSOL EM simulation program, where we use a single mode approach, with only the fundamental TE₀₁ mode being present in the entrance waveguide. In both cases we assume that the surface of the cavity (gold plated Si) is nearly lossless, and the additional apertures in the cavity needed to enclose the SiN legs (see Figure 3) are so small that radiation cannot leak into it. So we assume a cavity with only an entrance light-pipe, reflecting walls, and an absorbing film. Also we do not take into account the coupling mechanism of a horn or lens array to the entrance waveguide, but merely look at the absorption once the light has entered the cavity structure.

TABLE 1 PARAMETERS AND DIMENSIONS USED IN SIMULATING THE ABSORPTION EFFICIENCY OF A CAVITY ENCLOSED BOLOMETER WITH COMSOL.

Parameter	Value
Waveguide Width	100 μm
Waveguide Length	200 μm
Thickness of top wafer	200 μm
Cavity width at widest point	382.84 μm
Absorber Width	200 μm
Absorber Surface Resistance	377 Ω/\square
Absorber thickness	20 nm

We have analyzed several different configurations of pyramidal shaped cavities. Some initial results are shown in Figure 8 and Figure 10. More detailed analysis of this structure will be published elsewhere. An example of a ray-tracing simulation is shown in Figure 8. In this initial simulation the absorber size was equal to the dimension of the waveguide entrance (100x100 μm) and the largest dimension of the cavity was 400x400 μm . Therefore the absorbing film fills only a relatively small area of the cross section of the cavity. Even with this configuration we find that due to the

many internal reflections an absorption efficiency of 85% can be obtained.

An initial result of a COMSOL simulation is shown in Figure 10. The parameters that were used in this simulation are shown in TABLE 1. These numbers are chosen to comply with the restrictions on pixel size and spacing for the development of the far-infrared TES bolometers developed for the SAFARI instrument. The SAFARI instrument has three wavelength bands covering the 30-200 μm wavelength range (2-9 THz). Standard wafer thicknesses of Si wafers, and the capabilities of DRIE etching match well with the required dimensions in these far-infrared wavelengths. In this initial design of the pyramidal cavity we observe that the absorption has a cut-on frequency at 1.5 THz due to the $100 \times 100 \mu\text{m}$ waveguide, shows a strong resonant behavior between 1.5 to 3 THz and then has a more than 80% coupling efficiency up to 9 THz (where we stopped our simulation) with some notable resonances between 5 and 7 THz. To get rid of these

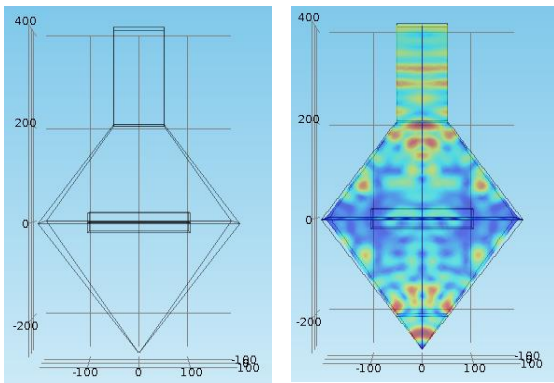


Figure 9 COMSOL modelling of a pyramidal cavity with a thin film absorber. The dimensions in the figures are in μm . On the right the electric field distribution within the cavity at a frequency of 5.3 THz. The waveguide is exited with the fundamental TE01 mode.

resonances we have further optimized the cavity design by introducing some asymmetry that smears out the resonances. By doing so we are able to get a simulated response of the cavity coupled bolometer over a very wide band running from 2-9 THz, only limited by the cut-on frequency of the waveguide, and the end frequency of our simulation.

V. CONCLUSION

In conclusion we have described the possible configuration of a silicon micro-machined cavity coupled bolometer that can be used in the far-infrared wavelength range. Simulations show that the design can have broadband coupling over a very wide wavelength range. Compared to existing designs that make use of a combination of Si bolometer wafers and Cu reflecting backshorts or cavities, the use of Si micro-machined cavities has several advantages with respect to vertical alignment, packing density, and thermal expansion properties at cryogenic temperatures. A more detailed study on the simulated performance will be published elsewhere.

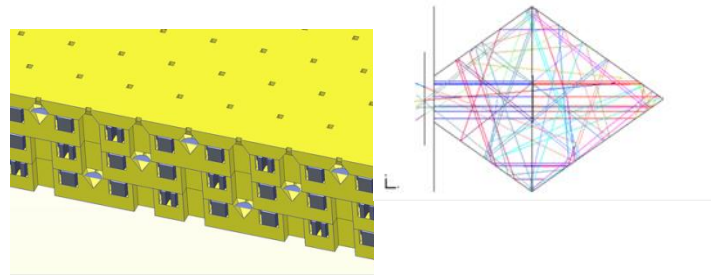


Figure 8 Ray tracing simulations of a pyramidal cavity enclosed bolometer. The ray tracing results for only a few rays are shown and it can be seen that rays that enter the cavity perpendicular to the absorber are reflected many times within the cavity, due to the 70.6 degree angle of the pyramid. Based on simulations with many more rays it is shown that an absorption efficiency of 85% can be achieved.

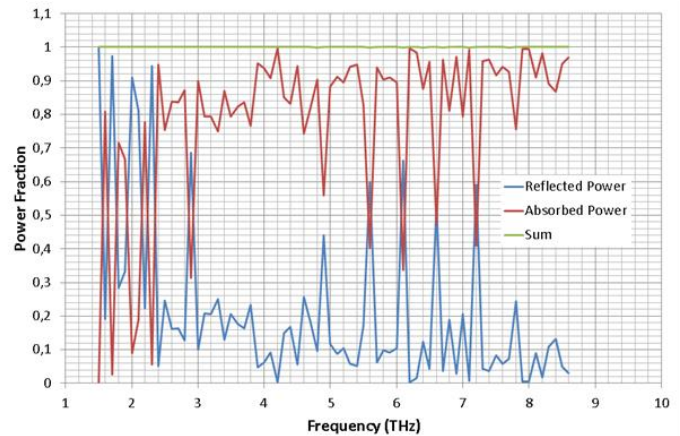


Figure 10 absorbed (red), reflected (blue) and total power (green) of the simulated cavity shown in Fig 9. The absorbed power is measured within the thin film, the reflected power is measured at the input port of the waveguide. The summation is used to cross-check the simulation. The waveguide has a cut-on at 1.5 THz. In the region where the cavity is not very much over-moded, strong resonant behavior is observed.

REFERENCES

- [1] Irwin, K. D. and Hilton, G. C., "Transition-edge sensors," [Cryogenic Particle Detection], C. Enss, Ed., Springer, 81-97 (2005)
- [2] Jackson, B., de Korte, P., van der Kuur, J., Mauskopf, P., Beyer, J., Bruijn, M., Cros, A., et al. IEEE Transactions on Terahertz Science and Technology 2(99), 1-10 (2011).
- [3] Michael D. Audley ; Gert de Lange ; Jian-Rong Gao ; Pourya Khosropanah ; Marcel Ridder, et al. Proc. SPIE 8452, Millimeter, Submillimeter, and Far-Infrared Detectors and Instrumentation for Astronomy VI, 84520B (September 27, 2012); doi:10.1117/12.925234
- [4] Holland W. S. et al., 2013, MNRAS, 430, 2513.
- [5] J.W. Henning, P. Ade, K.A. Aird, J.E. Austermann, J.A. Beall, D. Becker, B.A. Benson, L.E. Bleem, J. Britton, J.E. Carlstrom et al. Proc.SPIE Int.Soc.Opt.Eng. 8452 (2012) 84523A
- [6] P.L. Richards and M. Tinkham, Phys. Rev.119, 575 (1960).
- [7] D. A. Harper, R. H. Hildebrand, R. Stiening, and R. Winston Applied Optics, Vol. 15, Issue 1, pp. 53-60 (1976)
- [8] G.T.A.
- [9] Kovacs, N.I. Maluf, and K.E. Petersen, "Bulk Micromachining of Silicon," IEEE Proceedings, vol. 86, no. 8, pp. 1536-1551, August 1998
- J.A. Murphy and R. Padman, Infrared Physics, Vol 31, No 3, pp 291-299, 1991.